Determining the air-void content of hardened concretes using tactile sensing

Kucukkalfa, Eyuphan; Holthuizen, Patrick E.; Çopuroğlu, Oğuzhan; Schlangen, Erik; Fotouhi, Mohammad

DOI
10.58286/31735

Publication date
2025

Document Version
Final published version

Published in
e-Journal of Nondestructive Testing

e-Journal of Nondestructive Testing - ISSN 1435-4934 - www.ndt.net

NDT-CE 2025 - The International Symposium
on Nondestructive Testing in Civil Engineering
Izmir, Türkiye, September 24-26, 2025

Determining the air-void content of hardened concretes using tactile sensing

Eyuphan KUCUKKALFA[1], Patrick HOLTHUIZEN[1], Oguzhan COPUROGLU[1], Erik SCHLANGEN[1], Mohammad FOTOUHI[1]

[1] Faculty of Civil Engineering & Geosciences, Delft University of Technology,
Delft, The Netherlands; E.Kucukkalfa@tudelft.nl, P.E.Holthuizen@tudelft.nl, O.Copuroglu@tudelft.nl,
Erik.Schlangen@tudelft.nl, M.Fotouhi-1@tudelft.nl

Abstract

Accurate evaluation of air-void content in hardened concrete is important for assessing durability and long-term performance. Traditional methods often require time-consuming surface preparation and depend on imaging techniques that are sensitive to surface texture. This study investigates the potential of a high-resolution tactile sensing approach for non-destructive void detection with minimal surface preparation. To understand the effect of surface roughness, void detection was first performed on paired concrete specimens with identical internal surfaces, while one was left unpolished and the other polished. Despite the presence of surface irregularities, the tactile sensor was still able to identify most of the voids larger than a defined threshold, demonstrating its effectiveness even under challenging surface conditions. In the second phase, the sensor's void quantification performance was benchmarked on a polished specimen using a standardized digital microscopy-based method. The tactile system estimated porosity at 4.58% with an average void area of 0.013 mm², closely matching the reference digital microscopy-based results of 5.05% and 0.011 mm². These results highlight the sensor's capability to produce consistent and quantitative measurements on both rough and smooth surfaces. The approach offers a practical alternative to traditional void analysis methods, with the potential to simplify inspection workflows and support future automation in concrete surface evaluation.

Keywords: Air-void content, hardened concretes, polishing, imaging, tactile sensing

1. Introduction

Accurate characterization of hardened concrete surfaces is essential for evaluating material performance, predicting long-term durability, and maintaining structural integrity [1]. Among the critical surface features, air-void content plays a crucial role due to its strong correlation with properties such as permeability, freeze-thaw resistance, and compressive properties [2,3]. Traditional non-destructive testing (NDT) methods, including ultrasonic pulse velocity, impact-echo, and ground-penetrating radar (GPR), have been employed for concrete evaluation; however, these techniques often lack the spatial resolution required for surface-level analysis and can be highly sensitive to surface roughness or material inhomogeneity [4,5].

Quantification of air voids has relied on laboratory procedures, such as polishing hardened concrete specimens followed by optical imaging and stereological analysis based on ASTM C457 [6,7]. Even though the capacity of achieving high accuracy through void content measurements, these techniques are time-consuming and highly dependent on operator expertise [8]. Furthermore, concrete is a heterogeneous composite material composed of components with varying hardness and reflectivity, such as aggregates and cement paste, making proper surface preparation essential for reliable measurements [9,10]. In the absence of a standardized surface preparation protocol, the repeatability and objectivity of these traditional techniques are compromised. Achieving a consistent surface quality suitable for quantitative analysis is especially challenging in field or large-scale testing scenarios.

These challenges emphasize a clear gap in the current state-of-the-art about the need for an NDT method that can perform quantitative surface-level porosity assessment without

 https://doi.org/10.58286/31735

destructive preparation. While, remaining robust under variable lighting, material compositions, and surface textures, this method also need to deliver high-resolution topographic data suitable for objective and repeatable void classification.

To address this need, this study introduces an application of the GelSight tactile sensor for air-void evaluation on concrete surfaces. GelSight is a portable, high-resolution 3D tactile sensor that captures micron-scale surface topography through direct contact, without being affected by visual features such as surface gloss or ambient light [11,12]. Unlike conventional image-based systems, GelSight can scan unpolished concrete surfaces without prior preparation, making it highly suited for in-situ inspection and rapid implementation.

The main goal of this work is to develop a reliable, non-destructive, and user-friendly method for detecting and measuring air voids in concrete. Using multi-scale filtering the study introduces a classification approach based on tactile heightmap data. This removes the need for manual segmentation, making the process more consistent and easier to apply.

By comparing polished and unpolished specimens, the study also shows how surface texture can affect the accuracy of void detection and porosity results. This approach supports the development of practical and scalable NDT methods for concrete inspection. The tactile sensing technique shows strong potential both as a supporting tool and as a fast, repeatable solution for surface evaluation in lab and on-site conditions.

2. Materials and Methods

The experimental programme was structured into two sequential phases. Phase 1 examined how surface roughness affects tactile sensor accuracy using split concrete cores, with one half left unpolished and the other polished. Upon confirming the sensor's reliability, Phase 2 involved measurements on a separate specimen specifically prepared for void content analysis in accordance with current standards. In this phase, tactile measurements were taken at random locations on the polished surface to quantify air void content and compare it with results obtained using the standard contrast-enhanced image analysis method.

2.1 Materials and Sample Preparation

The concrete specimens for roughness assessment were extracted from an existing structural component, representing the surface conditions typically encountered in aged infrastructure. As illustrated in Figure 1.a, cylindrical cores of standard dimensions were extracted and subsequently split into two halves. One half was retained as unpolished specimen, while the other was subjected to a systematic grinding and polishing procedure to obtain a smooth surface.

Surface preparation of the polished specimen was conducted using a Struers LaboPol-60 grinding and polishing machine under wet conditions. Silicon carbide (SiC) abrasive papers with standardized FEPA P-grade grit sizes were employed throughout the process. The grinding was performed at a constant speed of 300 rpm, with the specimen positioned near the perimeter of the rotating disc to ensure a uniform and reproducible scratchy action. The sample position remained fixed during all grinding steps. After each step, the specimens were cleaned using an ultrasonic bath with demineralized water and dried with an air gun to eliminate residual slurry or debris.

The polishing sequence began with coarse P180 grit ($D_{50} \approx 82$ µm) and progressed through increasingly finer grits, ending with P1200 ($D_{50} \approx 15.3$ µm). In total, six grit sizes were used, with each applied in two sub-steps by rotating the specimen orientation by 90°, resulting in twelve grinding steps, as adapted from prior work [9]. Each step was maintained for one minute to ensure consistent material removal and minimize surface anisotropy introduced by directional abrasion. This standardized procedure enabled the preparation of a well-polished surface suitable for high-resolution tactile sensing, while the unpolished counterpart provided a realistic benchmark for evaluating performance under field-representative surface conditions.

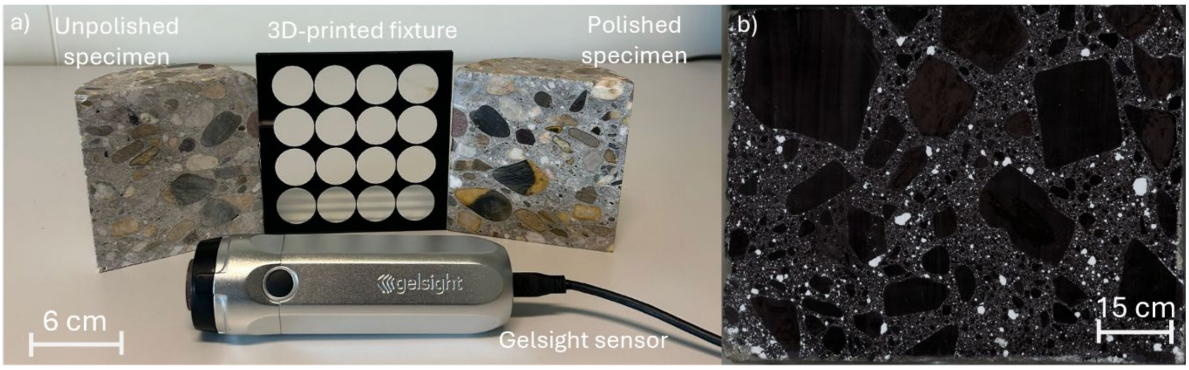

Figure 1: a) Experimental setup used to investigate the effect of surface roughness on measurement accuracy, and b) digital microscopy image of a sample prepared for void content analysis.

Void content analysis was conducted in accordance with ASTM C457/C457M–24 using the contrast-enhanced image analysis method. The surface was first polished using a multi-step grinding sequence to obtain a smooth and reflective finish. To enhance contrast, the polished surface was coated with a thin layer of black permanent ink, and white powder was lightly applied so that it settled only inside air void. A high-resolution digital microscopy image shown in Figure 1.b was captured under uniform lighting. The image was converted to 8-bit grayscale, thresholded, and binarized in ImageJ. Finally, the void content was calculated as the ratio of white pixel area to the total image area.

2.2 Tactile Measurements

Tactile surface measurements were conducted using the GelSight Mobile™ Series 2, a high-resolution, non-destructive 3D surface characterization device. This handheld sensor captures fine surface deformations by imaging the contact interface through a soft elastomeric membrane. The system converts tactile impressions into high-fidelity 3D heightmaps, enabling micron-scale surface analysis in the X, Y, and Z dimensions [13]. With a field of view of 17.0 mm × 14.2 mm and sub-micron vertical resolution (<1 µm), it is particularly suited for characterizing heterogeneous surfaces such as concrete.

In Phase 1, a custom 3D-printed fixture seen in Figure 1.a was employed to ensure consistent spatial alignment across both the unpolished and polished halves of the split specimens. Sixteen predefined scanning windows were distributed across the fixture to capture representative surface features. This configuration enabled direct side-by-side comparison of surface roughness effects on sensor measurements.

In Phase 2, the sensor was applied to a specimen in Figure 1.b, which is prepared for void content analysis. Tactile measurements were performed at randomly selected locations on the polished surface to capture 3D topography and estimate void content. The resulting heightmaps were processed to extract porosity metrics and were compared against results obtained according to current standard method.

2.3 Methodology

This section details the computational pipeline for analysing the surface heightmaps obtained from tactile scans, aiming to quantify the void content in hardened concrete samples. The workflow involves spatial calibration, multi-scale filtering, adaptive thresholding to accurately detect and measure surface voids.

The heightmap data obtained from tactile scanning of the concrete surface was used to calculate the void content of the hardened samples. To avoid noise from the physical boundaries and to improve the accuracy of filtering, 5% was cropped from each edge of the original heightmap. The spatial resolution of the cropped data was preserved, and meshgrid matrices were generated along the X and Y directions. Using the physical resolution in both directions ($dx \times dy$), the pixel area was calculated as $A_p = dx \cdot dy$, which was used as a base for volume calculation.

To remove high-frequency noise and detect voids at different scales, multi-scale Gaussian smoothing was applied [14]. This approach was necessary to detect both small and large voids, since a single smoothing scale may only highlight features of a specific size. A fine-scale Gaussian filter with standard deviation σ=2 was used to enhance small voids, and a coarse-scale filter with σ=8 was used to detect larger ones. After smoothing, the original surface was subtracted from the smoothed versions to create detrended surfaces. The negative deviations on these surfaces were considered potential voids.

Adaptive thresholding was then applied on each detrended map. Threshold values were calculated based on the mean (μ) and standard deviation (σ) of each map using the Equations 1 and 2.

$$T_{fine} = \mu_{fine} - 2\sigma_{fine} \tag{1}$$

$$T_{coarse} = \mu_{coarse} - \sigma_{coarse} \tag{2}$$

Binary masks from both fine and coarse scales were combined to form a single void mask. The combined mask was further improved using advanced morphological operations. Small noise regions with fewer than 30 pixels were removed. The final void mask was used along with the original heightmap to calculate the total void area and volume. The void volume was calculated by multiplying the negative height values of the void pixels with the pixel area, and summing over all void pixels, as shown in Equation 3. This method allows accurate and balanced detection of both small and large voids, providing a reliable estimation of the total void content in the concrete surface.

$$V_{void} = \sum_{(i,j)\in mask} |h_{i,j}| \cdot A_p \tag{3}$$

3. Results and Discussion

This section presents the experimental findings obtained from the tactile sensing-based void detection approach and its comparison with conventional imaging techniques. The analysis was conducted in two phases: first, to assess the effect of surface roughness on detection accuracy, and second, to benchmark the void quantification performance against a standardized void content calculation method. The results aim to evaluate the feasibility, strengths, and limitations of the tactile sensing system in capturing void characteristics relevant to structural health monitoring applications.

3.1 Effect of the Surface Roughness on Void Detection

Phase 1 aimed to explore the influence of surface roughness on the void detection capability of the tactile sensing system. Split cylindrical concrete cores were utilized, where each half represented the same internal surfaces of unpolished and polished sides. This allowed a direct comparison of the tactile sensor's performance on surfaces with differing roughness levels, as illustrated in Figure 2.

Figure 2a shows the tactile sensing and digital microscopy results from the unpolished specimen, while Figure 2b displays the same region from the polished counterpart. The difference in surface texture is visually apparent in both grayscale tactile images and in the digital microscopy outputs.

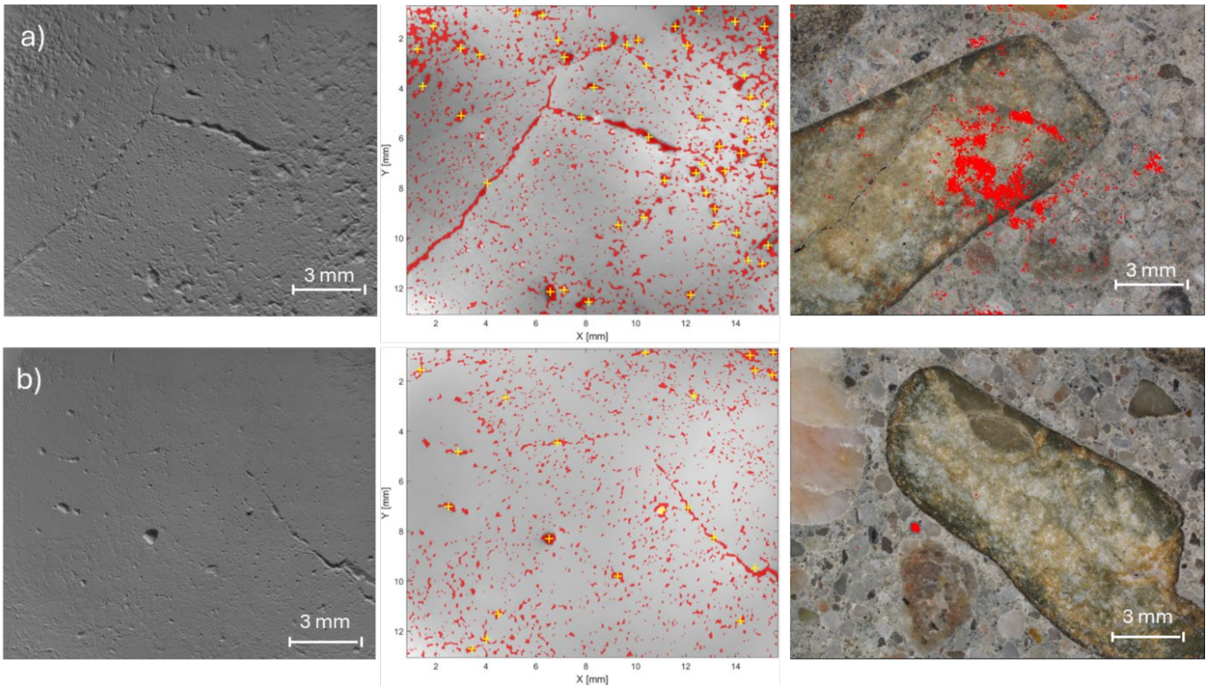

Figure 2: Representative grayscale tactile image and corresponding void detection output, shown alongside digital microscopy-based depth analysis of the same region from opposite sides of the specimen: a) unpolished surface, and b) polished surface after cross-sectioning.

A clear effect of roughness on void detection is observed. For the unpolished specimen, the surface irregularities introduce significant noise into the depth data, making it difficult to distinguish between actual voids and rough texture. This is particularly evident in the digital microscopy image of the unpolished sample, where void-like depressions and random surface pits overlap, leading to poor segmentation accuracy. Without following a standardized preparation procedure, digital microscopy-based void analysis on such rough surfaces yields unreliable results due to the absence of reliable 3D profile data.

On the other hand, tactile sensing demonstrates resilience to surface irregularities by utilizing heightmap-based analysis. Even on the rough surface, the tactile sensor was able to detect prominent voids, including those larger than 0.3 mm in diameter, as marked in yellow in the second column of Figure 2a and 2b. The benefit of direct topographical sensing becomes especially clear when comparing results from the polished surface, where the smoother texture provides a cleaner height signal that reduces false positives and improves the clarity of void boundaries.

The tactile sensor captures the effect of roughness and shows promising potential in identifying critical voids even on non-ideal surfaces. These findings support the feasibility of tactile sensing as a complementary or alternative method for structural void characterization, particularly in field conditions where specimen polishing is not always practical. In the next phase, a specimen prepared in accordance with ASTM standards was evaluated to benchmark the sensor's quantification accuracy under ideal surface conditions.

3.2 Void Content Calculation

A comparative void content analysis was conducted following void content measurement standard and a tactile sensing approach. The goal was to evaluate the capability of the tactile sensing method in detecting voids by benchmarking it against a standard imaging-based porosity measurement technique. Accordingly, porosity percentage and average void area were calculated for both approaches.

Figure 3a shows the segmented image acquired from digital microscopy, covering an area of 100.17 mm × 76.65 mm. The segmentation process highlights the voids within the concrete specimen, enabling quantitative porosity analysis. The calculated porosity using this method was 5.05%, with an average void area of 0.011 mm² and a standard deviation of 0.047. The significant spread in void area suggests the presence of both small and relatively larger voids distributed throughout the scanned region.

Figure 3b displays a representative grayscale tactile image captured from a randomly scanned region of the reference surface. The tactile sensing method is capable of capturing detailed surface topology variations associated with subsurface voids. The corresponding void detection output is shown in Figure 3c, where red dots indicate identified voids, and yellow markers highlight voids larger than 0.3 mm in diameter. This automated detection process yielded a porosity estimate of 4.58%, with an average cell area of 0.013 mm² and a standard deviation of 0.003.

Overall, both methods showed a consistent level of porosity in the sample, with minor differences attributable to resolution limits and sensitivity differences between the techniques. In the case of digital microscopy, porosity quantification relies heavily on the resolution of the captured image and the thresholding parameters used during image segmentation. The accuracy of void detection is particularly sensitive to the threshold value that separates voids from the region of interest, which can vary depending on lighting conditions, surface finish, and material heterogeneity. Moreover, obtaining a high-resolution scan of the entire specimen surface typically requires segmenting the surface into multiple image tiles, followed by stitching and processing which makes the process time-consuming and labour-intensive.

In contrast, the tactile sensing method offers a more efficient and potentially scalable alternative. It enables high-resolution surface profiling in a much shorter time, with less dependency on lighting or surface colour contrast. Because the sensing is based on direct surface deformation capture, it can more consistently detect fine surface depressions caused by subsurface voids, even in cases where contrast-based methods might struggle. Furthermore, the ability of the tactile system to rapidly identify voids underscores its promise as a practical tool for in-situ structural health monitoring. Although further refinement of the scanning and post-processing algorithms is still possible, these results demonstrate the strong potential of tactile sensing as a viable alternative or complementary method to traditional image-based void analysis.

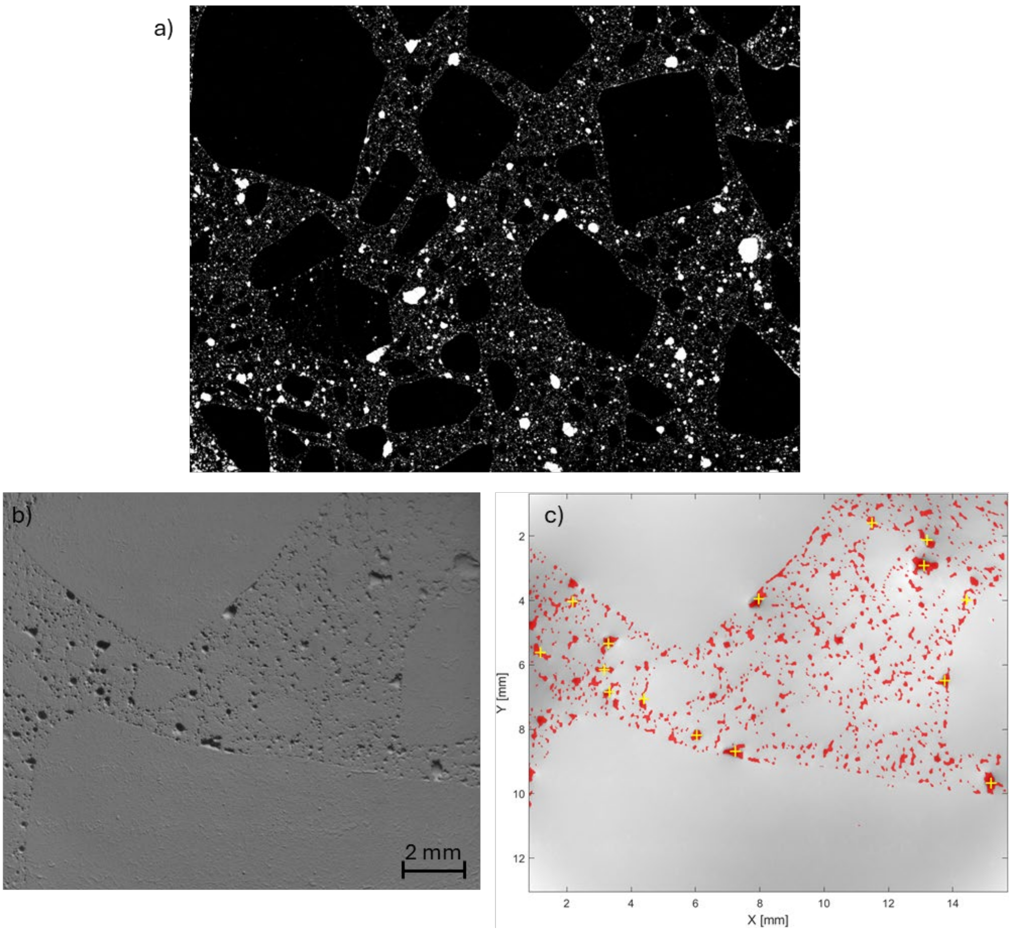

Figure 3: (a) Segmented digital microscopy image of the specimen for void content analysis (100.17 mm × 76.65 mm); (b) representative grayscale tactile image from a randomly scanned reference surface; (c) void detection output, with yellow marks indicating voids larger than 0.3 mm in diameter.

4. Conclusions

This study demonstrated the feasibility of using a high-resolution tactile sensing system for non-destructive void detection and quantification on concrete surfaces. Through a two-phase experimental approach, the system's performance was evaluated on both polished and unpolished specimens and benchmarked against a standardized digital microscopy-based porosity analysis. Results showed that surface roughness has a significant impact on void detection accuracy, particularly for image-based methods. While digital microscopy struggles on unpolished surfaces due to segmentation noise and inconsistent depth data, tactile sensing maintains reliable performance by directly capturing surface topography. Even in the presence of surface irregularities, the tactile sensor successfully identified critical voids, demonstrating resilience to roughness-induced noise.

In the porosity benchmarking phase, tactile sensing produced void metrics that closely matched those of the conventional method, with comparable porosity percentages and average void areas. This consistency highlights the potential of tactile sensing as a reliable tool for quantitative analysis.

The system offers practical advantages such as portability, independence from lighting conditions, and rapid data acquisition without requiring extensive specimen preparation. However, its current rule-based detection strategy still depends on predefined geometric

thresholds, which could limit its generalizability across varied materials or defect types. Future improvements may focus on incorporating adaptive or data-driven classification approaches to enhance robustness and automation.
In summary, the results support tactile sensing as a reliable, scalable, and field-adaptable alternative to conventional imaging techniques, particularly valuable for structural health monitoring applications where fast and reproducible surface inspection is essential.

References

[1] H Ma et al., 'Establishment of the Concrete Simulated Void System Using CT Images', JOM, Vol. 77, No. 7, pp. 5526–5541, April 2025, doi: https://doi.org/10.1007/s11837-025-07380-5.
[2] M Krstic et al., 'Freeze–thaw resistance and Air-void analysis of concrete with recycled glass–Pozzolan using X-ray micro-tomography', Materials, 14(1), 154, 2020.
[3] X H Zeng et al., 'Investigation on air-voids structure and compressive strength of concrete at low atmospheric pressure', Cement and Concrete Composites, 122, 104139, 2021.
[4] H Taheri, S Hedjazi, and M Spears, 'Practical Assessment of Non-Destructive Testing (NDT) Techniques for On-Site Application of GDOT Projects (No. FHWA-GA-25-2105)'. Georgia. Dept. of Transporation, Office of Performance-Based Management and Research, 2025.
[5] J Pandum, K Hashimoto, T Sugiyama, and W Yodsudjai, 'Impact-echo for different level cracks detection in concrete with artificial intelligence based on un/supervised deep learning', Construction and Building Materials, 487, 142080, 2025.
[6] ASTM International, 'Standard Test Method for Microscopical Determination of Parameters of the Air-Void System in Hardened Concrete: C 457/C 457M-24', ASTM, 2024.
[7] P C Fonseca and G W Scherer, 'An image analysis procedure to quantify the air void system of mortar and concrete', Materials and Structures, Vol. 48, No. 10, pp. 3087–3098, August 2014. doi: https://doi.org/10.1617/s11527-014-0381-9.
[8] J Tao et al, 'Automated image segmentation of air voids in hardened concrete surface using photometric stereo method', International Journal of Pavement Engineering, 23(14), 5168-5185, 2022.
[9] P Holthuizen and O Çopuroğlu, 'Quantification of surface grinding during the sample preparation of cementitious materials by optical profilometry', Journal of Microscopy, vol. 294, no. 2, pp. 128–136, December 2023, doi: https://doi.org/10.1111/jmi.13256.
[10] K Scrivener, R Snellings, and B Lothenbach, 'A Practical Guide to Microstructural Analysis of Cementitious Materials', CRC Press, 2016.
[11] W Yuan, S Dong, and E Adelson, 'GelSight: High-Resolution Robot Tactile Sensors for Estimating Geometry and Force', Sensors, Vol. 17, No. 12, p. 2762, November 2017, doi: https://doi.org/10.3390/s17122762.
[12] T Mantel, J Rohaly, and M K Johnson, '3d surface topography measurement using elastomeric contact'. 11th International Symposium on NDT in Aerospace, 2019.
[13] 'GelSight Mobile™ Series 2', https://www.gelsight.com/products.
[14] P Cao, Z Min, and L Zhenchun, 'Adaptive Filtering De-noising Method Based on Generalized S-Transform and Gaussian Smoothing', International Geophysical Conference, Beijing, China, Society of Exploration Geophysicists and Chinese Petroleum Society, 2018.